Decay modes of analog states studied by the (^{3}He, dp) reaction

G. Finkel, D. Ashery, and A. I. Yavin
Department of Physics and Astronomy, Tel Aviv University, Israel

A. Boudard, G. Bruge, A. Chaumeaux, and M. Rouger
C.E.N. de Saclay, France

(Received 4 August 1978)

The (^{3}He, dp) reaction was studied at 30-MeV bombarding energy on ^{60}Ni, ^{62}Ni, and ^{90}Zr. Protons were detected in coincidence with deuterons at various angles, in and out of the reaction plane. Angular correlations were measured between the deuterons populating analog states and the protons associated with the decay of the analog states to several states in the final nucleus. Spectroscopic information is derived from the analysis of the measured angular correlations on ten analog states: three in ^{61}Cu, four in ^{63}Cu, and three in ^{91}Nb.

[NUCLEAR REACTIONS ^{60,62}Ni, ^{90}Zr(^{3}He, dp), E=30.2 MeV; measured coincidence $\sigma(E_d, E_p, \theta_p)$. Deduce spectroscopic information IAS in ^{61,63}Cu, ^{91}Nb. Enriched targets. Calculate angular correlation function.]

I. INTRODUCTION

A state $|\psi\rangle^{J^\pi}$ in an odd-A nucleus may be described in the weak coupling model as a nucleon in a single-particle state coupled to an even-even core in the (0^+) ground state or in an excited state. This configuration can be written in the form

$$|\psi\rangle^{J^\pi} = \alpha|\psi_c(0^+)\,\psi_N(l,j)\rangle^{J^\pi} + \beta|\psi_c(2^+)\psi_N(l_1,j_1)\rangle^{J^\pi} + \gamma|\psi_c(2^+)\psi_N(l_2,j_2)\rangle^{J^\pi} + \cdots, \quad (1)$$

where ψ_c is the core-state wave function and ψ_N is the single particle wave function. Only one orbital angular momentum quantum number l is allowed for the nucleon when the core is in a 0^+ state, while more l values are allowed if the core is in a state with higher angular momentum, subject to the limitations imposed by parity and angular momentum conservation rules.

The coupling of the nucleon to the core ground state can be measured by studying stripping reactions, such as (d, p) or (^{3}He, d), on the core nucleus as a target. These measurements yield the value of the spectroscopic factor α^2. When the state which is studied is the ground state of a stable nucleus, the other coefficients in Eq. (1) may be measured in pick-up reactions such as (p, d) or ($d, ^3$He). For other states (i.e., excited states and ground states of unstable nuclei) this information may be obtained through the study of the decay properties of analog states, which are unbound to nucleon emission. For states which can be described as neutrons coupled to an even core, the analog states will have the same structure, but with a proton replacing the neutron in the parent states, and coupled to the same core. Information on the various coefficients in Eq. (1) may then be obtained by studying the proton decay modes of the analog states.

The decay properties of analog states have been investigated by two methods: (1) Studies of resonance ($p, p'\gamma$) reactions have been carried out on a number of nuclei[1,2] and yielded very valuable information. These studies have been performed on each analog state individually and are generally limited to states populated through small ($l \leq 2$) angular momentum transfers. (2) The analog states have been populated by a direct (^{3}He, d) reaction, and the decay protons ($\tilde{p}$) have been detected in coincidence with the outgoing deuterons. Several states are studied simultaneously in this method and states reached through large angular momentum transfer are strongly populated. The two methods may be considered, to some extent, as complementary. Yet more parameters are measured in the ($p, p'\gamma$) experiment and the deduced information is, therefore, more complete.

Two early studies of the (^{3}He, $d\tilde{p}$) reaction, in which only qualitative information was obtained, have been reported.[3,4] This reaction has been studied more recently[5,6] on Ti and Cr isotopes and yielded more detailed information. In the present work the (^{3}He, $d\tilde{p}$) reaction has been studied on the ^{60}Ni, ^{62}Ni, and ^{90}Zr isotopes. Protons have been detected in coincidence with deuterons in various angles, in and out of the reaction plane, and spectroscopic information has been obtained for 10 analog states: three in ^{61}Cu, four in ^{63}Cu and, three in ^{91}Nb.

The experimental procedure used in the present work is described in Sec. II and the results are

given in Sec. III. In Sec. IV we describe the method used for the analysis of the angular correlation in order to obtain information on the decay modes of the analog states. A model dependent analysis of the structure of the analog states is given in Sec. V and the results are discussed in Sec. VI. More details on the calculation of the angular correlation function are given in the Appendix.

II. EXPERIMENTAL PROCEDURE

A 30.2-MeV ^{3}He beam from the C.E.N.-Saclay cyclotron was used to bombard isotopically enriched ^{60}Ni, ^{62}Ni, and ^{90}Zr targets. The thicknesses and enrichments of the targets are listed in Table I. The outgoing deuterons were detected at a fixed angle (25° for the Ni targets and 30° for the ^{90}Zr target) with a $\Delta E - E$ silicon detector telescope (600 μ and 3000 μ) coupled to a Chaivre-type[7] particle-identifier system. The protons, which decay from the residual nuclei, were measured with a silicon detector, 450 mm^2 in area, and 500 μ in thickness. A similar detector was placed behind these detectors, and served to reject protons with energy greater than 8 MeV.

A time-to-amplitude converter unit (T.A.C.) served as the coincidence unit between deuterons and protons. A typical time spectrum is shown in Fig. 1. The peaks labeled 1, 2, and 4 represent random coincidence events of protons and deuterons from two different beam bursts. The peak labeled 3 contains true coincidence events as well as random coincidence ones, all from the same beam burst. The coincidence spectra were stored, in the memory of a P.D.P.-8 computer, as matrices of 128×256 channels. The data were collected by gating on peak number 3, but some spectra were also taken by gating on the other peaks and used to correct the data for random coincidences. These random spectra were found to be evenly distributed over the matrix so that the correction was small. A monitor detector, set at a fixed angle in the scattering plane, was used to trigger a pulser whose pulses were fed through all the electronic system and stored in the matrix. A proper dead-time correction was then performed with this procedure. The "singles"-deuteron spectrum from the (^{3}He, d) reaction was collected simultaneously with the coincidence spectrum and stored separately. The dead-time correction in the singles spectrum was performed by the same method.

TABLE I. Target thicknesses and enrichments.

Target isotope	Thickness (μg/cm^2)	Enrichment (%)
^{60}Ni	170	95
^{62}Ni	130	95
^{90}Zr	620	97.7

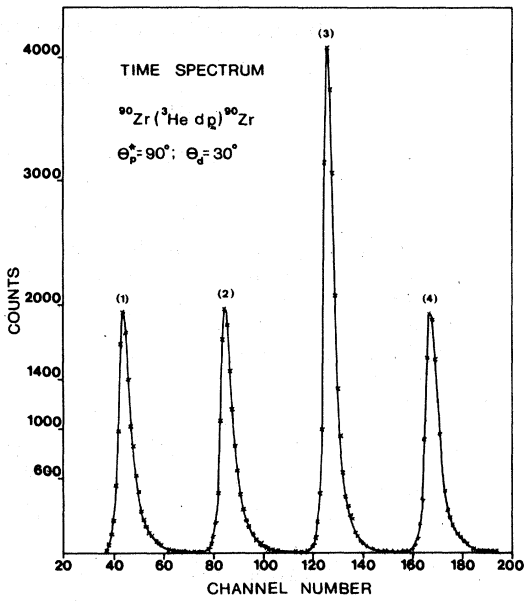

FIG. 1. Spectrum of time-to-amplitude converter between the deuteron and proton detector. θ_p^* is the angle between the beam direction and the proton detector.

A geometrical arrangement for angular correlation measurements, for which the correlation functions are available in simplified forms[8] requires that the deuterons should be detected at 0° or 180°. Due to the experimental difficulties in setting a detector at 0° and the very low cross section for the (^{3}He, d) reaction at 180°, we chose a different experimental arrangement. The deuteron detector was set at an angle at which the ratio between the yield from the (^{3}He, d) reaction[9,10] and the total counting rate (due mainly to elastic scattering) is optimal. Protons were then detected at various angles in the reaction plane. The proton angle is defined as the angle between the proton direction and the direction of the compound nucleus, which recoils after the (^{3}He, d) reaction. The direction of the recoiling nucleus is determined from the kinematics. Proton measurements were taken at 10 angles for ^{60}Ni, 3 angles for ^{62}Ni, and 4 angles for ^{90}Zr.

The angular correlation does not necessarily have an azimutal isotropy in this arrangement. Measurements of the coincidence spectrum with the proton detector set out of the reaction plane thus became necessary. The proton detector was then mounted on a cone with an opening angle of 22°, whose symmetry axis coincided with the direction of the recoiling nucleus (Fig. 2). Four measurements were then taken at $\theta_p = 22°$ and azimuthal angles $\phi_p = 0°, 50°, 90°, 130°$. These measurements were carried out only on the ^{60}Ni target.

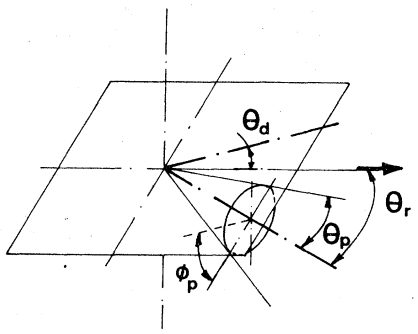

FIG. 2. Schematic diagram of the experimental setup.

III. EXPERIMENTAL RESULTS

A typical deuteron-proton coincidence spectrum (formed with some channel regrouping) is displayed in Fig. 3. The data points are seen to concentrate along kinematic bands, each associated with a particular state in the final nucleus. The width of the kinematic bands is determined by the energy resolution in each detector. The energy calibration was done for the deuteron detector with the singles-deuteron spectrum and for the proton detector with α sources. The calibration was checked against the kinematic band associated with the ground state of the final nucleus. The kinematic bands for the other states and for the ^{12}C and ^{16}O contaminants are extracted from three-body-kinematics calculations and are shown as lines in the spectra. Whenever the proton angle is changed the positions of the kinematic bands are changed. A larger displacement occurs for the bands associated with the light contaminants. One consideration in the choice of proton angles was to avoid overlapping of kinematic bands from the contaminants and the target. When a line perpendicular to the kinematic bands is drawn in the spectrum and the data are projected on this line, the energy spectrum of the final nucleus (including the contaminants) is obtained. Some projections of this kind are displayed in Fig. 4.

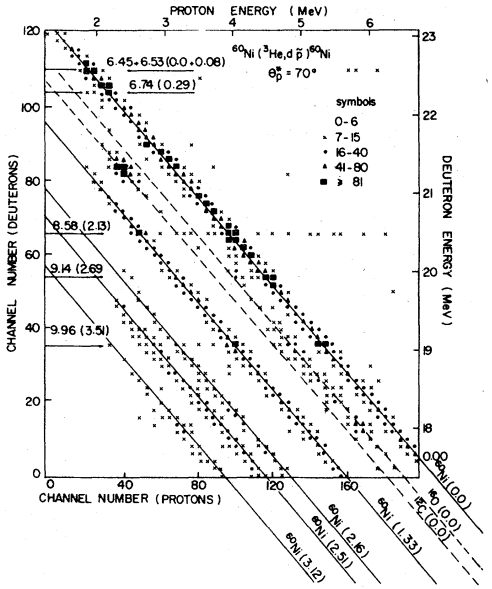

FIG. 3. Deuteron-proton coincidence spectrum for the ^{60}Ni(^{3}He, $d\tilde{p}$) ^{60}Ni reaction. θ_p^* is the angle between the beam direction and the proton detector.

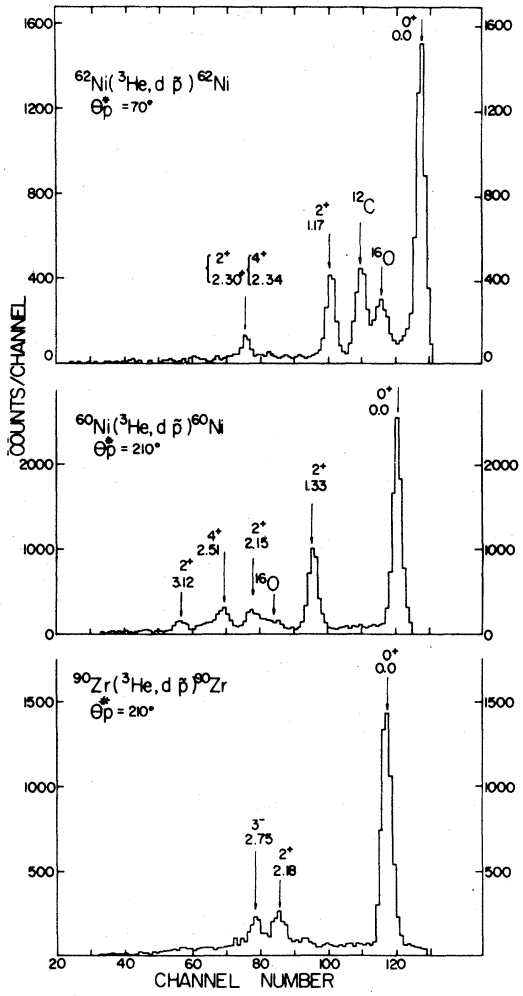

FIG. 4. Projections of the coincidence spectra on the energy axis of the residual nucleus. θ_p^* is the angle between the beam direction and the proton detector.

Each kinematic band was projected on the deuteron energy axis and spectra of these projections are shown in Figs. 5–7. The peaks in a spectrum of this kind represent the decay from different analog states to a single state (characterized by the selected band) in the final nucleus. The singles-deuteron spectrum from the (^{3}He, d) reaction,

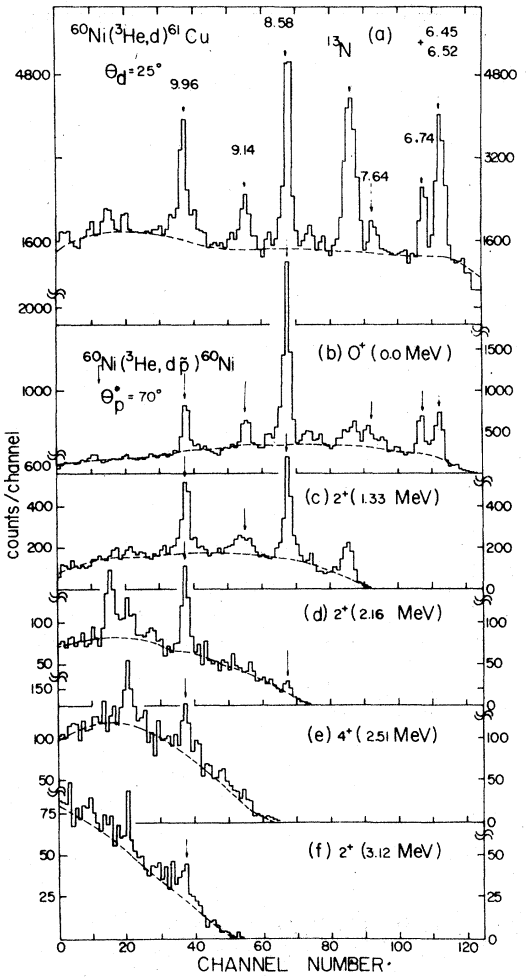

FIG. 5. (a) Singles deuteron spectrum from the ^{60}Ni(^{3}He,d)^{61}Cu reaction. (b)-(f) Projections of the kinematic bands in the coincidence spectrum of the ^{60}Ni(^{3}He, $d\tilde{p}$)^{60}Ni reaction on the deuteron energy axis. The dashed line indicates the assumed background. θ_p^* is the angle between the beam direction and the proton detector.

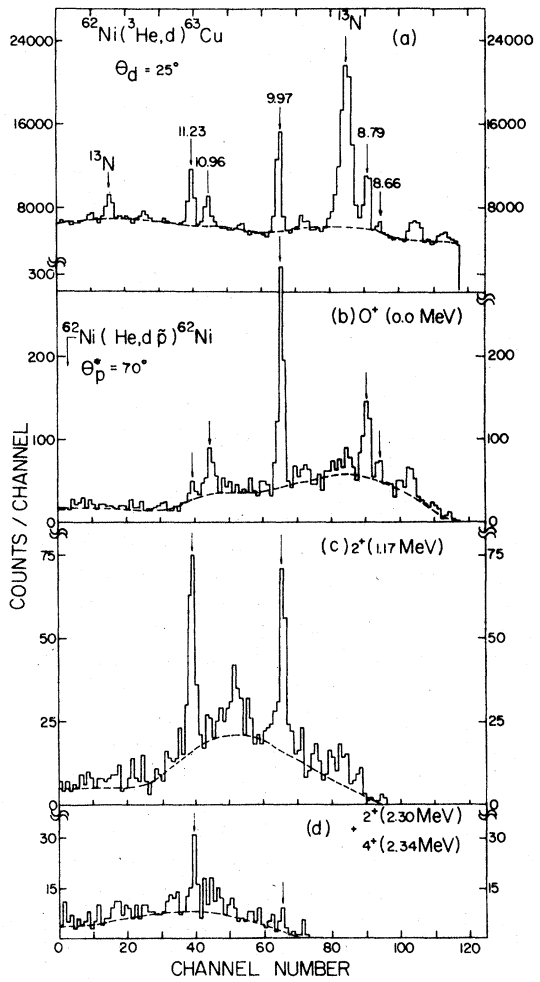

FIG. 6. (a) Singles deuteron spectrum from the ^{62}Ni(^{3}He,d)^{63}Cu reaction. (b)-(d) Projections of the kinematic bands in the coincidence spectrum of the ^{62}Ni(^{3}He, $d\tilde{p}$)^{62}Ni reaction on the deuteron energy axis. The dashed line indicates the assumed background. θ_p^* is the angle between the beam direction and the proton detector.

which was measured simultaneously, appears in the upper part of Figs. 5–7. Each peak in the projection spectra was integrated. A smooth background was assumed in this integration. The number obtained was corrected for dead time and for random coincidences. Although the total number of random coincidence events is quite large (Fig. 1), these events are distributed almost evenly over the whole matrix and their contribution to the bands is therefore small. When this procedure is repeated for all proton angles, the deuteron-proton angular correlation is obtained.

The results of the measured angular correlations in the reaction plane are given in Figs. 8–11. Only statistical errors are indicated in Figs. 8–11. The systematic errors are estimated to be about 12%, coming mainly from uncertainties in background subtraction. The double-differential cross section in normalized unit is given by

$$\frac{d^2\sigma}{d\Omega_d d\Omega_p}\ (\text{normalized units}) \equiv W_{\exp}(\theta, \phi) = \frac{N_{\text{coin}}(\theta, \phi)}{N_{\text{sing}}} \cdot \frac{4\pi}{\Delta\Omega_p} . \quad (2)$$

N_{sing} here is the total number of times a certain analog state was populated and is obtained from the singles deuteron spectrum. The value N_{coin} is obtained from the deuteron-proton coincidence spectrum and is the number of decays of the same analog state to one state in the final nucleus, detected at a particular angle. This value is calculated for the center of mass system. $\Delta\Omega_p$ is the solid angle

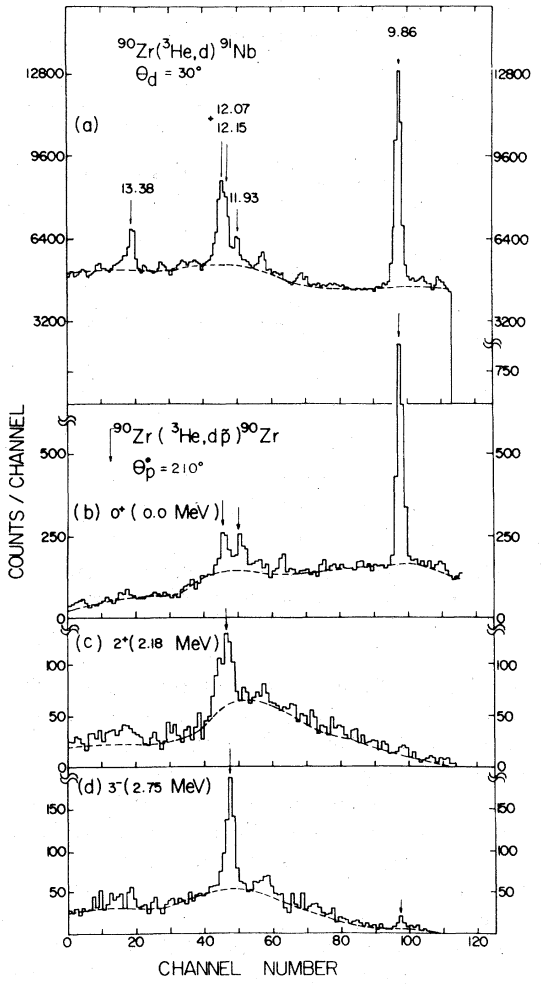

FIG. 7. (a) Singles deuteron spectrum from the ^{90}Zr(^{3}He,d)^{91}Nb reaction. (b)-(d) Projections of the kinematic bands in the coincidence spectrum of the ^{90}Zr(^{3}He, $d\tilde{p}$)^{90}Zr reaction on the deuteron energy axis. The dashed line indicates the assumed background. $\theta_{\tilde{p}}^*$ is the angle between the beam direction and the proton detector.

subtended by the proton detector. When the angular correlation is integrated with this normalization, over all angles, and then summed over the decays to all the states (f) in the final nucleus, the following equation should hold:

$$\frac{1}{4\pi}\sum_f \int_{\phi=0}^{2\pi}\int_{\theta=0}^{\pi} W_{\exp}(\theta,\phi)\sin\theta d\theta d\phi = 1 .$$

The same procedure, applied to the measurements taken for ^{60}Ni with the proton detector set out of the reaction plane, yields the azimuthal angular correlation displayed in Fig. 12. The lines drawn in Figs. 8–12 are results of the angular correlation calculations discussed in Sec. IV.

Some of the analog states, which are populated in the reaction, appear as unresolved doublets.

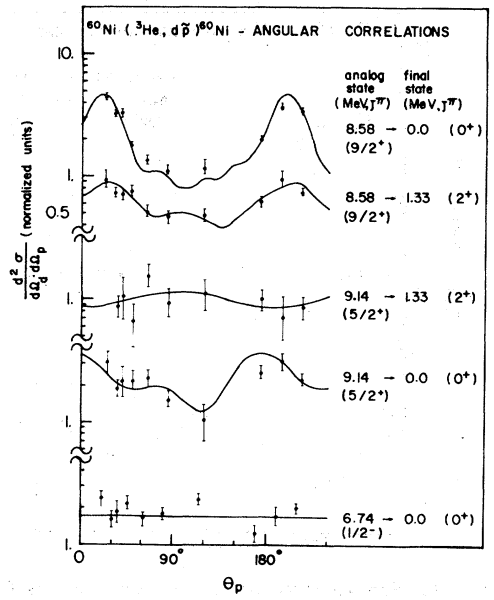

FIG. 8. Proton-deuteron angular correlations for the ^{60}Ni(^{3}He,$d\tilde{p}$)^{60}Ni reaction measured in the reaction plane.

These states were not analyzed. For all the states that were analyzed, a measurable decay was observed only to the ground state (0^+) and first excited state (2^+) of the final nucleus and all the angular correlations displayed in Figs. 8–12 are therefore associated only with these two states. The sole exception is the 11.23 MeV state in ^{63}Cu for which decay to the second excited state in ^{62}Ni was also observed. However, this final state is itself an unresolved doublet [2.30 MeV, (2^+) and 2.34

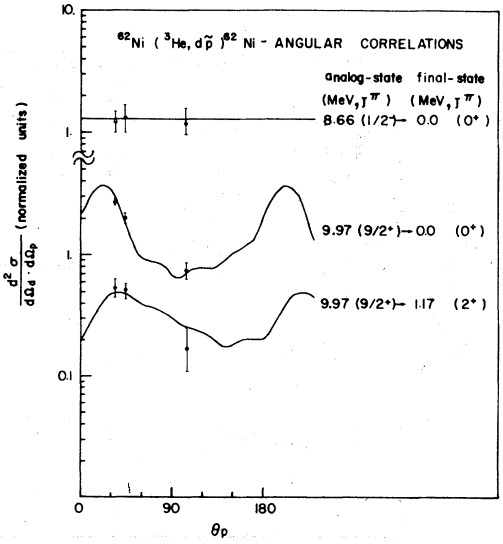

FIG. 9. Proton-deuteron angular correlations for the ^{62}Ni(^{3}He,$d\tilde{p}$)^{62}Ni reaction measured in the reaction plane.

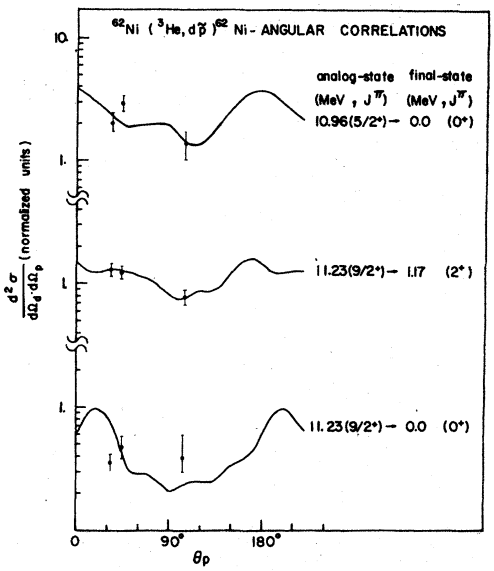

FIG. 10. Proton-deuteron angular correlations for the ^{62}Ni(^{3}He,$d\tilde{p}$)^{62}Ni reaction measured in the reaction plane.

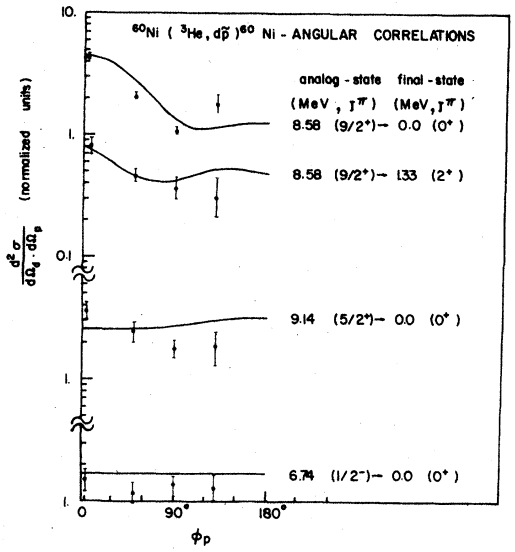

FIG. 12. Proton-deuteron angular correlations for the ^{60}Ni(^{3}He,$d\tilde{p}$)^{60}Ni reaction measured outside the reaction plane.

MeV (4⁺)] and therefore this particular transition could not be analyzed.

IV. ANALYSIS OF THE ANGULAR CORRELATIONS

The experimental setup used in the present work does not match any of the standard geometries, for which simplified formalisms for the analysis of the angular correlation were developed.[8] The projectile and the outgoing particles all had nonzero spins, and neither 0° nor 180° could be used as detection angles. Therefore, the most general formalism of angular correlation analysis had to be employed and adapted to the configurations used in this work. The shape of the angular distribution of the outgoing protons had to be calculated and fitted with the measurements, which are carried out at several angles. Then the angular distribution had to be integrated over all angles, in order to evaluate the total decay width for each final state.

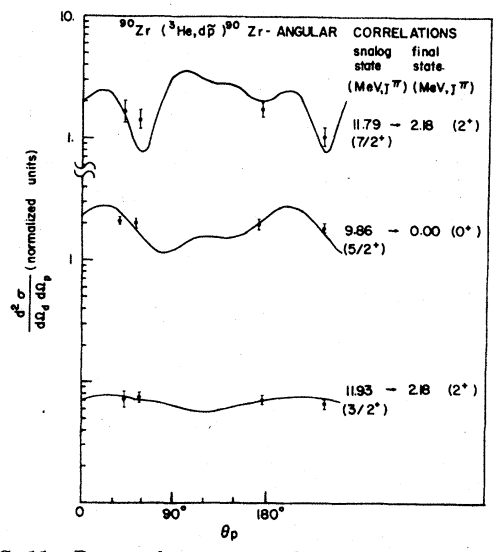

FIG. 11. Proton-deuteron angular correlations for the ^{90}Zr(^{3}He,$d\tilde{p}$)^{90}Zr reaction measured in the reaction plane.

Details on the calculation of the angular correlation between the outgoing deuteron and proton are given in the Appendix. We will state here only the main results. The angular correlation function is given by

$$W(\theta,\phi)=\sum_{i,f}\left|\sum_{n}A_{i\to n}\cdot A_{n\to f}\right|^2, \tag{3}$$

where i, n, and f are the initial, the intermediate, and the final states, respectively, as defined in the Appendix. The amplitudes $A_{i\to n}$ for the population of the analog state are calculated with the computer code DWUCK,[11] which has been modified[9,10,12] for the treatment of unbound states. The parameters used in this calculation are listed in Table II. The amplitudes $A_{n\to f}$ for the proton decay of the analog state are given by two different expressions. In the case where the decay is to the 0⁺ (ground state) of the final nucleus, the outgoing proton can carry only one value of angular momentum l and the amplitude is given by

$$A_{n\to f}(m_s)=\sum_{m_p}(l\,m_l s m_s|j_p m_p)\cdot Y^{l}_{m_l}(\theta,\phi). \tag{4}$$

Details on the notation and the calculations are

TABLE II. Parameters used for DWBA calculations.

	Target	V_R	W	W_S	V_{SO}	r_{0R}	a_R	r_{01}	a_1	r_{0c}	λ	Ref.
^{3}He	Ni	−180.0	−19.0			1.14	0.71	1.54	0.78	1.25		14
	Zr	−157.77	−11.71			1.174	0.706	1.596	1.032	1.25		15
d	Ni	−96.31		50.52	6.37	1.119	0.735	1.261	0.842	1.25		16
	Zr	−100.8		52.56	6.53	1.099	0.835	1.344	0.747	1.25		16
p	Ni, Zr					1.20	0.65			1.25	25	17

given in the Appendix.

When the decay is to the first excited ($J_c = 2^+$) state, several l values are allowed, but their number can usually be reduced to only two values, l_1 and l_2, as discussed in Sec. VI. In these cases, when D denotes the relative amplitude for decay with angular momentum value l_1, the decay amplitude is given by

$$A_{n\to f}(m_c, m_s) = \sum_{m_j} [D(l_1 m_{l_1} s m_s | j_{p_1} m_{p_1})(j_{p_1} m_{p_1} J_c m_c | J m_J) \cdot Y^{l_1}_{m_{l_1}}(\theta, \phi) + (1 - D^2)^{1/2}(l_2 m_{l_2} s m_s | j_{p_2} m_{p_2})(j_{p_2} m_{p_2} J_c m_c | J m_J) \cdot Y^{l_2}_{m_{l_2}}(\theta, \phi)] \ . \quad (5)$$

For transitions to the 0^+ ground state there is no adjustable parameter which affects the shape of the calculated angular correlation, and the only parameter used to fit the calculation with the experimental results is the overall normalization. For transitions to the 2^+ excited state the (complex) relative amplitude D, which affects the shape of the angular correlation function, has first to be fitted to the data, and then the overall normalization is obtained. All the fits were done by the least-square method.

The calculated angular correlations, in the reaction plane, are shown as lines in Figs. 8–11. As can be seen the agreement between the calculations and the data is good as can be best seen in the case of ^{60}Ni (Fig. 8), where the number of measured data points is relatively large. Even in the isotropic $\frac{1}{2} \to 0^+$ transition only 4 out of 10 points deviate from the straight line by as much as 2 standard deviations which is accepted statistically. Values of the amplitude D, which were deduced from analysis of these angular correlation measurements, are given in Table III. The measured transitions proceed either through $l_1 = 2$ and $l_2 = 0$

TABLE III. Decay-mode amplitudes, branching ratios, and ratios of total decay rates to population rates.

Nucleus	Analog state Excitation energy (MeV)	J^π	D $l_1=4$ (D_R, D_I)	D $l_2=2$ $(1-D^2)^{1/2}$	D $l_1=2$ (D_R, D_I)	D $l_2=0$ $(1-D^2)^{1/2}$	Branching ratio 0^+ (%)	Branching ratio 2^+ (%)	$\frac{N(\text{decay})}{N(\text{pop})}$
^{61}Cu	6.74	$\frac{1}{2}^-$					>99	<1	1.63 ± 0.25
	8.58	$\frac{3}{2}^+$	(−0.05, 0.5)	0.87			69 ± 10	31 ± 7	1.48 ± 0.3
	9.14	$\frac{5}{2}^+$			(0.0, 0.05)	~1	60 ± 10	40 ± 8	2.42 ± 0.5
^{63}Cu	8.66	$\frac{1}{2}^-$					>99	<1	1.28 ± 0.2
	9.97	$\frac{3}{2}^+$	(−0.6, 0.65)	0.47			81 ± 13	19 ± 4	1.04 ± 0.2
	10.96	$\frac{5}{2}^+$					>95	<5	1.57 ± 0.25
	11.23	$\frac{3}{2}^+$	(−0.05, −0.95)	0.32			23 ± 5	67 ± 12	0.93 ± 0.2
^{91}Nb	9.86	$\frac{5}{2}^+$					>99	<1	1.17 ± 0.2
	11.79	$\frac{7}{2}^+$	(−0.25, −0.15)	0.95			10 ± 3	90 ± 13	1.73 ± 0.4
	11.93	$\frac{3}{2}^+$			(0.2, −0.75)	0.63			

or through $l_1=4$ and $l_2=2$. For l_1 we present both real and imaginary values of D with typical uncertainties of ±0.1, arising from the fitting procedure and the optical model calculations. For l_2 we give the value $(1-D^2)^{1/2}$.

The results of the angular correlation measurements out of the reaction plane, in units which are defined in Sec. III [Eq. (2)], are shown for the ^{60}Ni target in Fig. 12. Here $\theta_p=22°$ and ϕ_p is the angle between the detected proton and the reaction plane, as defined in Fig. 2. The calculated angular correlations, shown as lines in Fig. 12, do not have any adjustable parameters. The angular momentum amplitude D and the overall normalization are those which were obtained from the fit to the data in the reaction plane. The good agreement between the calculations and the measured results serves as a check of the validity of the calculations, and indicates that measurements out of the reaction plane may not be necessary. Such measurements were not repeated for ^{62}Ni and ^{90}Zr.

The other nuclear parameters, which are obtained from the present work, are the decay branching ratios of the analog states. These are the partial decay widths to the ground state $[\Gamma(0^+)/\Gamma]$ and to the first excited state $[\Gamma(2^+)/\Gamma]$.

In order to obtain the branching ratios for a particular analog state, the angular correlation of the decay protons to each final state has to be integrated over all angles. Since the measured angular correlation $W_{\rm exp}(\theta,\phi)$ is not sufficient for this integration, the integration is performed on the calculated angular correlation function $W_{\rm th}(\theta,\phi)$ and the measured data are used to get a normalization constant N:

$$W_{\rm exp}(\theta,\phi)=NW_{\rm th}(\theta,\phi)\ . \tag{6}$$

The integral

$$I=\frac{1}{4\pi}\int\int W_{\rm exp}(\theta,\phi)\sin\theta d\theta d\phi$$
$$=\frac{N}{4\pi}\int\int W_{\rm th}(\theta,\phi)\sin\theta d\theta d\phi \tag{7}$$

gives the total decay of the analog state to one state in the final nucleus. The branching ratios $I(0^+)/[I(0^+)+I(2^+)]$ and $I(2^+)/[I(0^+)+I(2^+)]$ are listed in Table III. When the integrals I for the two states in the final nucleus are added together the total decay rate of the analog state is obtained. This is so since for all the analog states studied in this work proton emission is the only allowed particle decay channel, and the gamma decay widths are relatively very small and can be neglected. The population rate for the analog states is measured from the singles deuteron spectrum. The ratio between the measured decay rate $N_{\rm decay}$ and population rate $N_{\rm pop}$ is listed in Table III. This ratio is found, unexpectedly, to be greater than unity and this result is discussed in Sec. VI. The errors in the values shown in Table III include statistical errors, uncertainties in the fitting procedure, and experimental systematic errors. The errors include also an estimated contribution due to uncertainties in the optical model parameters, which gave a typical error of 10% in the values of $A_{i\to n}$.

V. STRUCTURE OF THE ANALOG STATES

The data presented in this work may be used in order to understand the structure of the analog states which were studied. This must be done in the framework of a nuclear model. One way of interpretation is to describe the analog state, in the weak coupling model, in the following way:

$$|\text{Analog state}\,\psi\rangle^{J^\pi}=\alpha|\psi_c(0^+)\psi_p(l,j_p)\rangle^{J^\pi}$$
$$+\beta|\psi_c(2^+)\psi_p(l_1,j_{p_1})\rangle^{J^\pi}$$
$$+\gamma|\psi_c(2^+)\psi_p(l_2,j_{p_2})\rangle^{J^\pi}+\cdots, \tag{8}$$

where a proton is coupled to the core ψ_c. If the core is in a 0^+ state the proton can have only one l and j_p value. When the core is in a state with higher angular momentum value, such as 2^+, the proton can have several l and j_p values consistent with angular momentum and parity conservation. In practice, proton decays will not consist of more than two l values, since the probability for transitions with larger angular momentum values will be greatly reduced by their smaller penetrability.[13] This matter is further discussed in Sec. VI.

The coefficient α^2, which describes the overlap between the analog state and the ground state of the final nucleus, is the spectroscopic factor. It is obtained from the population of the analog state by the (^{3}He, d) stripping reaction on the final nucleus as a target. This reaction was investigated[9,10] on all nuclei and analog states involved in the present work, and the values of α^2 for each analog state are taken from these studies. The transitions to the 2^+ state in the final nucleus are analyzed through the angular correlation of the decay protons, as discussed in Sec. IV. The square of the amplitude D, which describes the relative intensity of a proton transition with angular momentum l_1 is given by

$$D^2=\frac{\beta^2 f(l_1,E_p)}{\beta^2 f(l_1,E_p)+\gamma^2 f(l_2,E_p)}\ , \tag{9}$$

where $f(l_1,E_p)$ and $f(l_2,E_p)$ are the penetrabilities multiplied by $(2l+1)$ for the protons decaying from

the analog state to the final 2^+ state with energy E_p and angular momentum values l_1 and l_2, respectively. This gives us one relation with two unknowns, β and γ. One way to obtain a second relation is to assume that in Eq. (8) the coefficients α, β, and γ give a complete description of the structure of the analog state. This assumption is plausible for analog states which are considered to have simple structures. In such a case we have $\alpha^2+\beta^2+\gamma^2=1$, and the values of β and γ can thus be determined.

VI. DISCUSSION

The spectroscopic information derived from analysis of the angular correlation is presented in Table IV. The uncertainty of the quoted spectroscopic factors is within the normally accepted uncertainty of distorted wave Born approximation (DWBA) calculation. For each analog state, the spectroscopic factor α^2 for the ground state transition is taken from studies of the (^{3}He, d) reaction.[9,10] The spectroscopic factors β^2 and γ^2 for the (2^+) excited state transition are obtained from the results of the present work as discussed in Sec. V, and are given for the two l values relevant to each transition. These two values are selected according to the following considerations:

(1) The only negative parity analog states observed have a J^π value of $\frac{1}{2}^-$. The formation of such a state by coupling the 2^+ core to a proton is limited to protons in the $p_{3/2}$ or $f_{5/2}$ configurations.
(2) The observed positive parity analog states may be formed by coupling the 2^+ core to a proton in the $s_{1/2}$, $d_{3/2}$, $d_{5/2}$, $g_{7/2}$, and $g_{9/2}$ configurations, i.e., $l=0$, 2, and 4. In most cases these possibilities are reduced to only two by angular momentum conservation. In the few analyzed cases, where this reduction does not occur, we assumed that only the two smaller l values have significant contribution to the transition, the largest one being practically inhibited by penetrability.[13] Whenever the transition is dominated by one l value, the error in its spectroscopic factor is determined by the precision in α^2 (taken usually to be about 20%). When two l values have comparable contributions (^{91}Nb, $\frac{7}{2}^+$ and $\frac{9}{2}^+$ states), the error in the spectroscopic factors is determined by D^2. For these two transitions the error was found to be 30%. We will now make a few comments concerning each analog state.

TABLE IV. Deduced spectroscopic factors.

Nucleus	Excitation energy MeV	J^π	0^+	2^+ $l=0$	2^+ $l=2$	2^+ $l=4$
^{61}Cu	6.74	$\frac{1}{2}^-$	0.65			
	8.58	$\frac{9}{2}^+$	0.46		0.03	0.51
	9.14	$\frac{5}{2}^+$	0.16	0.84	<0.01	
^{63}Cu	8.66	$\frac{1}{2}^-$	0.39			
	9.97	$\frac{9}{2}^+$	0.48		<0.01	0.52
	10.96	$\frac{5}{2}^+$	0.30			
	11.23	$\frac{9}{2}^+$	0.22		0.01	0.77
^{91}Nb	9.86	$\frac{5}{2}^+$	0.96			
	11.79	$\frac{7}{2}^+$	0.11		0.41	0.48
	11.93	$\frac{3}{2}^+$	0.50	0.24	0.26	

A. ^{61}Cu

The 6.74-MeV state ($\frac{1}{2}^-$): the angular correlation measured for the decay of this state is isotropic, as expected for the decay of a spin $\frac{1}{2}$ state. From shell-model considerations and angular momentum conservation the state can be described as composed of a proton in the $p_{1/2}$ shell coupled to the (0^+) ground state, and protons in the $p_{3/2}$ and $f_{5/2}$ shells coupled to the (2^+) excited state. The ground state spectroscopic factor (0.65) implies that some coupling to an excited core state probably exists. However, the penetrability for a transition to the 2^+ state is extremely small due mainly to the low energy (0.56 MeV) available for this transition. This state must therefore decay predominantly to the ground state. No proton decay to the 2^+ state could be observed in this work due to the very low energy, below the threshold of the measurement.

The 8.58-MeV state ($\frac{9}{2}^+$): a weak decay with a branching ratio of the order of 1% is observed to the second excited state (2.16 MeV, 2^+) in ^{60}Ni. The angular correlation of the decay to the first excited state shows dominant contribution of $l=4$ transition. This would imply coupling of a proton in either the $g_{7/2}$ or $g_{9/2}$ shells to the 2^+ core. [It should be noted that another analog state, at 9.96 MeV, is known[9] to be populated through $l=4$ with a relatively small spectroscopic factor. Proton decays from this state were observed to five states in the final nucleus (see Fig. 5). This state is an unresolved doublet and it was not analyzed in detail.]

The 9.14-MeV state ($\frac{5}{2}^+$): although all the proton configurations mentioned above could be coupled to a 2^+ core to form a $\frac{5}{2}^+$ state, we assumed that $l=4$ decay will have only small contributions to the decay rate due to the relatively small penetrability. The angular correlation was analyzed assuming a mixed $l=0$ and $l=2$ transition and the major contribution is found to be from $l=0$. The doublets

at 6.5 MeV and the triplet at 7.64 MeV could not be analyzed.

B. ^{63}Cu

The 8.66-MeV state ($\frac{1}{2}^-$): the situation here is similar to that of the $\frac{1}{2}^-$ state in ^{61}Cu. Proton decay to the excited state could be observed experimentally, but this decay is suppressed, as compared to the ground state transition, by the much smaller penetrability (a factor of ≈500), and was not seen.

The 9.97 and 11.23-MeV states ($\frac{9}{2}^+$): for both states the decay to the 2^+ excited state in ^{62}Ni is dominated by $l=4$ transition. Due to sum-rule considerations this strength must be distributed between the $g_{7/2}$ and $g_{9/2}$ sub shells. The 11.23-MeV state decays also to the 2.3 MeV (2^+ and 4^+) doublet in ^{62}Ni with a branching ratio of about 10%.

The 10.96-MeV state ($\frac{5}{2}^+$): in spite of the small ground-state spectroscopic factor (0.3) no significant decay was observed from this analog state to the first and second excited states of ^{62}Ni. This could imply that the structure of this state includes configurations in which a proton is coupled to higher excited states in ^{62}Ni. A proton decay to such higher states would be suppressed by the small penetrability. The doublet at 8.79 could not be analyzed.

C. ^{91}Nb

The 9.86-MeV state ($\frac{5}{2}^+$) decays to the ground state of ^{90}Zr, with a spectroscopic factor $\alpha^2 = 0.96$.

The 11.79-MeV state ($\frac{7}{2}^+$): the spectroscopic factor for the ground-state transition is small (0.12). This state was observed to decay mainly to the 2^+ first excited state through $l=2$ and $l=4$ transitions, with comparable contributions.

The 11.93-MeV state ($\frac{3}{2}^+$): this is the only case where the agreement between the calculated and experimental angular correlation for the ground state transition is poor. For that reason a value for the branching ratio was not extracted. For the decay to the 2^+ state the agreement between experiment and calculation is good and this transition is found to proceed through $l=0$ and $l=2$ transitions, with comparable contributions.

The 12.07 MeV ($\frac{11}{2}^-$), and 12.15 MeV ($\frac{7}{2}^+$): although this doublet could not be analyzed we wish to mention that it decays with an appreciable branching ratio to the 2.75 MeV (3^-) state in ^{90}Zr.

For almost all the states studied, the total decay rate for all the transitions seems to exceed the rate at which the state is populated ($N_{\text{decay}}/N_{\text{pop}} > 1$, Table III). This conclusion is obviously incorrect, but the source for this puzzle is not clear. All the experimental sources for such a difference, e.g., solid angle, dead time correction, etc., were carefully checked and cannot provide a satisfactory explanation. It could be suggested that in spite of the good agreement with the experimental results, the calculated angular correlation is incorrect and leads to wrong results when integrated over all θ and ϕ angles. However, this reason cannot explain the effect for the spin $\frac{1}{2}$ states, where the angular correlation of the decay protons is isotropic, and we still find the same effect.

A possible explanation to this effect is that an interference exists between the analog state and the compound states in the continuum. The result of such an interference could be that in the coincidence spectra the background "under the analog states" should not be treated as being a smooth interpolation of the background in the vicinity of the state. If the decay is enhanced by contribution from the background, the observed effect could be explained.

The members of the Tel-Aviv University group are grateful to Dr. J. Thirion for his hospitality. We want to thank particularly H. Poussard and all the cyclotron crew for optimizing the beam during very long runs and B. Bricand who wrote all the on line computer programs. We are also grateful to Professor N. Auerbach and to Drs. M. Shuster and N. Spector for useful discussions.

APPENDIX: CALCULATION OF THE ANGULAR CORRELATION FUNCTION

We will evaluate the angular correlation function between the outgoing deuteron from the (^{3}He, d) reaction and the decay proton. It should be noted that in our experiment the angle of the deuteron detector was fixed, while the angle of the proton detector was varied. In its final form we describe the angular correlation as a function of the angle θ between the direction of the decay proton and the direction of the recoiling compound nucleus which subsequently emits the proton, and the angle ϕ between the proton direction and the reaction plane (Fig. 2). The angular correlation is given by

$$W(\theta,\phi)=\sum_{i,f}\left|\sum_{n}A_{i\to n}A_{n\to f}\right|^2, \tag{A1}$$

where i is the initial state, i.e., the target is in its (0^+) ground state and the ^{3}He projectile has spin projections $+\frac{1}{2}$ or $-\frac{1}{2}$. The intermediate state n is the nucleus formed by the (^{3}He, d) reaction in the analog state with a certain J^π value and projections m_J between $-J$ and $+J$, and the deuteron with its spin projection values of 0 and ±1. In the final state f we have the deuteron in the same states as in the intermediate state, the final nucleus with a spin and parity J_c^π and the projections M_c, and the

free proton with spin projections $\pm\frac{1}{2}$. The amplitudes $A_{i\to n}$ and $A_{n\to f}$ are for the transition from the initial to the intermediate state and from the intermediate to the final state, respectively. The summation is carried out on all the transitions between states which obey parity and angular momentum conservation rules. We will now discuss the evaluation of each of the transition amplitudes.

A. The amplitudes $A_{i\to n}$

These are the transition amplitudes for the (^{3}He, d) reaction. They are evaluated as a part of the DWBA calculations which are performed for this reaction. For this purpose we used the computer code DWUCK,[11] which was modified in order to be used for unbound states. Details of these modifications and the parameters used in the calculations have been published.[9,10,12] The transition amplitudes in these calculations are calculated for spin projections $m(^3\mathrm{He})=\pm\frac{1}{2}$, $m(d)=0,\pm1$ and for all the non-negative m_J values of the analog state. The amplitudes for transitions to states with negative m_J values are related to the amplitudes for transitions to states with the corresponding positive m_J value by a phase relation given by Satchler,[18]

$$(A_{i\to n})^{l,m,m_b,m_a}_{s,j}=(-1)^{m+j+l+s_b-s_a}(A_{i\to n})^{l,-m,-m_b,-m_a}. \tag{A2}$$

The notations are for a reaction $A(a,b)B$; s_a, s_b, m_a, and m_b are the spins and spin-projections for particles a and b, respectively. The other notations are defined by

$$\vec{j}=\vec{J}_B-\vec{J}_A,\quad \vec{s}=\vec{s}_a-\vec{s}_b,\quad \vec{l}=\vec{j}-\vec{s},$$
$$m=M_B+m_b-M_A-m_a. \tag{A3}$$

J_A, M_A and J_B, M_B are the spins and spin-projections of the target nucleus A and residual state B, respectively. From the modified code DWUCK and the phase relation (A2), we obtain the transition amplitudes $A_{i\to n}$ from the two initial states for which $[m(^3\mathrm{He})=\pm\frac{1}{2}]$ to all the intermediate states n.

B. The amplitudes $A_{n\to f}$

The transition amplitude $A_{n\to f}$ is given by

$$A_{n\to f}=\langle\psi_n|\psi_f\rangle, \tag{A4}$$

where ψ_n and ψ_f are the intermediate and final state wave functions, respectively. The final state wave function can be described by a product of the final nucleus wave function ψ_c and a free proton, namely,

$$\psi_f=\psi_c e^{i\vec{k}\cdot\vec{r}}\chi_{m_s}^{1/2}, \tag{A5}$$

where $\chi_{m_s}^{1/2}$ is the proton spin projection. The function $e^{i\vec{k}\cdot\vec{r}}$ can be expanded and we obtain for ψ_f the form

$$\psi_f=\psi_c(J_c,m_c)\chi_{m_s}^{1/2}4\pi \times\sum_{l=0}^{\infty}\sum_{m_l=-l}^{l} i^l j_l(k,r)Y^l_{m_l}(\theta,\phi)Y^{l*}_{m_l}(\Theta,\Phi), \tag{A6}$$

where θ and ϕ are the angles for the proton momentum $\hbar\vec{k}$ and Θ and Φ are the angles for the vector $\vec{r}$. The final nucleus wave function ψ_c is given for a spin J_c and projection m_c of the state in which the final nucleus is left after the proton decay.

The intermediate state wave function is described as a proton coupled to the core (J_c, m_c). We first discuss the case of the core being in a 0^+ state. In this case the proton can carry only one value of orbital angular momentum l and total angular momentum j_p, which are determined from the J^π values of the analog state. The intermediate state wave function then takes the form

$$\psi_n=\sum_{m_s,m_p}(lm_l sm_s|j_p m_p)Y^l_{m_l}(\Theta,\Phi)\chi_{m_s}^{1/2}\psi_c(0,0). \tag{A7}$$

s and m_s are the proton spin and spin-projection and m_p is the projection of the total angular momentum of the proton. The summation is carried out under the conditions

$$m_l+m_s=m_p,\quad -j_p\le m_p\le j_p. \tag{A8}$$

The final state wave function ψ_f is taken for a particular value of m_s. When we evaluate the transition amplitude for this case, according to (A4), we have (apart from a normalization factor)

$$A_{n\to f}=\sum_{m_p}(lm_l s\,m_s|j_p m_p)Y^l_{m_l}(\theta,\phi), \tag{A9}$$

when orthogonality relations were taken into account. If $J_c\neq0$ more l values are allowed, but the number of these values can be reduced by using shell model and penetrability considerations[13] (see Sec. VI). If we assume that only two l values contribute, l_1 and l_2, and denote by D the relative amplitude for a transition in which the proton carries orbital angular momentum l_1, the intermediate state wave function takes the form

$$\psi_n=D\Big[\sum_{m_s,m_{p_1},m_J}(l_1 m_{l_1} sm_s|j_{p_1}m_{p_1})(j_{p_1}m_{p_1}J_c m_c|Jm_J)Y^{l_1}_{m_{l_1}}(\Theta,\Phi)\chi_{m_s}^{1/2}\psi_c(J_c,m_c) +(1-D^2)^{1/2}\sum_{m_s,m_{p_2},m_J}(l_2 m_{l_2} sm_s|j_{p_2}m_{p_2})(j_{p_2}m_{p_2}J_c m_c|Jm_J)Y^{l_2}_{m_{l_2}}(\Theta,\Phi)\chi_{m_s}^{1/2}\psi_c(J_c,m_c)\Big]. \tag{A10}$$

j_{p_1} and j_{p_2} are the total angular momenta of a proton with an orbital angular momentum l_1 and l_2, respectively. The summations are carried out under the conditions

$$m_{l_1} + m_s = m_{p_1}, \quad m_{p_1} + m_c = m_J, \quad -J \leq m_J \leq J, \tag{A11}$$

and similarly for m_{l_2} and m_{p_2}. The transition amplitude now takes the form

$$A_{n\to f}(m_c, m_s) = \sum_{m_J} \Big[D(l_1 m_{l_1} s m_s | J_{p_1} m_{p_1})(J_{p_1} m_{p_1} J_c m_c | J m_J) Y^{l_1}_{m_{l_1}}(\theta, \phi) + (1 - D^2)^{1/2} (l_2 m_{l_2} s m_s | J_{p_2} m_{p_2})(J_{p_2} m_{p_2} J_c m_c | J m_J) Y^{l_2}_{m_{l_2}}(\theta, \phi) \Big] \tag{A12}$$

The angular correlation function is obtained when the transition amplitudes are inserted in expression (A1). When all summation indices are written explicitly this function will have (apart from a normalization constant) the form

$$W(\theta, \phi) = \sum_{m(^3\mathrm{He}) = -\frac{1}{2}}^{\frac{1}{2}} \sum_{m_d = -1}^{1} \sum_{m_s = -\frac{1}{2}}^{\frac{1}{2}} \sum_{m_c = -J_c}^{J_c} \Big| \sum_{m_J = -J}^{J} A_{i\to n}(m_{^3\mathrm{He}}, m_d, m_J) A_{n\to f}(m_c, m_s) \Big|^2 \tag{A13}$$

[1] E. Abramson, R. A. Eisenstein, I. Plesser, Z. Vager, and J. P. Wurm, Nucl. Phys. A144, 321 (1970).
[2] N. Cue, I. Plesser, Z. Vager, and G. F. Wheeler, Nucl. Phys. A229, 429 (1974).
[3] R. A. Hoffswell, D. Jammich, T. M. Noweir, and A. I. Yavin, Phys. Rev. Lett. 19, 754 (1967).
[4] D. Ashery, S. Alper, A. I. Yavin, J. P. Longequeue, D. Kong, A. Siou, and A. Giornia, Nucl. Phys. A179, 681 (1972).
[5] S. Gales, S. Fortier, H. Laurant, J. M. Maison, and J. P. Schapira, Nucl. Phys. A259, 189 (1976).
[6] S. Gales, S. Fortier, H. Laurant, J. M. Maison, and J. P. Schapira, Phys. Rev. C 14, 842 (1976).
[7] R. Chaminade, J. C. Faivre and J. Pain, Nucl. Instrum. Methods 49, 217 (1967).
[8] A. E. Litherland and A. J. Ferguson, Can. J. Phys. 39, 788 (1961).
[9] A. Boudard, G. Bruge, A. Chaumeaux, G. Finkel, D. Ashery, and A. I. Yavin, Phys. Rev. C 13, 1123 (1976).
[10] G. Finkel, D. Ashery, A. I. Yavin, G. Bruge, and A. Chaumeaux, Nucl. Phys. A217, 197 (1973).
[11] P. D. Kunz, University of Colorado, DWBA code DWUCK1967 (unpublished).
[12] D. Ashery, S. Alper, A. Moalem, Y. Shamai, A. I. Yavin, G. Bruge, A. Chaumeaux, and M. Moinester, Phys. Rev. C 5, 1729 (1972).
[13] For information on the dependence of the penetrability on energy and angular momentum, see, e.g., J. B. Marion and F. C. Young, *Nuclear Reaction Analysis* (North-Holland, Amsterdam, 1968).
[14] P. E. Rundquirt, M. K. Brussel, and A. I. Yavin, Phys. Rev. 168, 1287 (1968).
[15] R. L. Kozub and D. H. Youngblood, Phys. Rev. C 4, 535 (1971).
[16] C. M. Perey and F. G. Perey, Phys. Rev. 152, 923 (1966).
[17] D. J. Pullen and B. Rozner, Phys. Rev. 170, 1034 (1968).
[18] G. R. Satchler, Nucl. Phys. 55, 1 (1964).